

Quantifying Drought Impact on Wetland Vegetation in the Sacramento - San Joaquin Delta with Remote Sensing

Annemarie E. Peacock

ABSTRACT

A critical region for California's economy, drinking water supply, and wildlife, the Sacramento-San Joaquin Delta continues to face degradation and alteration. With current climate model projections, additional stressors such as drought are expected to impact this area further. Vegetation is crucial to the Delta's health, function, and provision of ecosystem services, and examining how Delta wetland vegetation responds to drought informs restoration and management priorities. In this study, I used remote sensing to quantify shifts in wetland vegetation across years of varying precipitation levels (average rainfall, 2009-2010; drought, 2011-2016; and after in 2017) to characterize drought impact on four wetland sites, two reference and two restored. Through supervised image classification, landscape metrics, and spectral vegetation indices, all sites significantly decreased in EVI and NDVI throughout the drought but showed unique trajectories in changes of vegetation land cover, patch characteristics, and general landscape metrics. The most recently restored site, Mayberry Farms, was characterized by highest landscape variability and increased vulnerability to drought.

KEYWORDS

GIS, Spectral Vegetation Indices, Change Detection, Landscape Metrics, NAIP

INTRODUCTION

Despite only accounting for an estimated 6% of global land cover, wetlands are one of the world's most productive and economically valuable ecosystems (Moreno-Mateos et. al 2012; IWMI 2014). They provide a multitude of ecosystem services including: biodiversity preservation, nutrient cycling, flood mitigation, water quality improvement, carbon sequestration, groundwater recharge and discharge, climate change mitigation, shoreline stabilization, nutrient and sediment retention, and recreation and tourism (Zedler and Kercher 2005). Wetlands are harbors of such high biodiversity because of their shallow water, high nutrient levels, and abundant primary productivity (Cloern et. al 2016). These features create favorable conditions for organisms such as fish, amphibians, insects, and larger organisms including birds and mammals that depend on wetlands for food, water, and shelter (Ramsar Convention 2013). In terms of direct human impact, wetlands are important sources of water, jobs, and food, such as agricultural and fishing industries (IWMI 2014). Wetlands are diverse and valuable ecosystems, but despite their immense ecological importance, they are facing widespread stress and degradation worldwide.

An important wetland area in California, the Sacramento-San Joaquin Delta (the Delta) is a river delta and estuary, beginning at the convergence of the Sacramento and San Joaquin Rivers, and this confluence extends over 3,000 square kilometers (Luoama et. al 2015). The Delta is a critical source of agricultural activity, water, and wildlife habitat in California; it provides drinking water for 22 million people, supports California's \$45 billion/year agricultural industry, and is home to over 750 species (Luoama et. al 2015; Hester et. al 2016). However, the Delta has faced significant alteration from its mid-19th century conditions (Cloern et. al 2016). Around 70% of the Delta has been converted to agriculture, and larger agricultural islands bordered by levees and waterways have mostly replaced the lower islands, shallow natural channels, and marshes of former wetlands (Luoama et. al 2015). Additionally, the Delta serves as a crucial water source in California, but draw on this resource has led to invasive management practices. Water drainage and levee construction to divert water and channel off agricultural areas has greatly altered the Delta from historic conditions (Luoama et. al 2015).

The Delta already experiences California's Mediterranean climate, which fluctuates between seasons and years, and recently, California experienced a severe drought from 2011 to 2016. Delta wetlands are complex ecosystems that receive water from a variety of sources

including Sierra Nevada snowpack runoff, tidal inundation, and water diversions for agriculture. Drought affects these water sources, and less precipitation decreases Sierra Nevada snowpack. This decrease initiates earlier snowmelt and higher winter runoff, which impacts input flow and leads to encroachment of salinity into freshwater areas of the Delta (Schile 2011).

In general, a wetland's hydrological conditions impact its vegetative structure and function. Changes in water source such as water drainage or drought, impact nutrient availability, soil characteristics, and sediment deposition, and changes in precipitation specifically can cause shifts in vegetation composition as a result of lower water depths and shorter inundation periods (Malone et. al 2015; US EPA 2002). Plants are particularly valuable indicators of wetland ecosystem health and function due to their relatively rapid growth rates and responses to environmental conditions (US EPA 2002). Therefore, tracking vegetation changes is an effective method to examine the effect of drought on wetland ecosystems. To measure vegetation density, growth, and type calculated spectral vegetation indices can be extracted from satellite imagery. The Normalized Difference Vegetation Index (NDVI) and Enhanced Vegetation Index (EVI) are vegetation indices ranging from -1.0 to +1.0 that describe greenness, or vegetative density, biomass, and health based on an area's spectral properties. In addition, satellite imagery can be classified and used for post-classification comparisons to quantify and analyze shifts in the area and distribution of wetland vegetation.

In general, many unknowns remain about drought-associated changes in wetland ecosystem vegetation, including how drought affects plant health, coverage, and on what timescale these changes are observable and harmful to the ecosystem, and if certain site characteristics or management practices increase drought impact (Touchette et. al 2009). California is more likely to experience drought if lower precipitation co-occurs with warmer temperatures, and anthropogenic warming will continue to increase this probability. If dry years are also warm: evaporation increases, insufficient water is stored as winter and spring snowpack, and runoff and in soil moisture experience changes that impact water availability and riparian habitats and species (Diffenbaugh et. al 2015). In the interest of mitigating widespread wetland degradation and loss, many wetland restoration and preservation efforts are being explored in the Delta, and effective wetland management and restoration require understanding of vegetation drought responses. Tracking drought impact is particularly important as the Delta faces additional stressors from climate change. With many climate change models forecasting increases in drought severity and

duration in places like California, it is important to understand how drought affects a wetland's capacity to fulfill key ecosystem functions or meet restoration objectives (Touchette et. al 2009).

Therefore, to quantify effects of drought on different wetland ecosystems, I used spectral indices and image classification to examine how wetland vegetation was impacted by different precipitation in the Sacramento-San Joaquin Delta between years of normal precipitation (2009-2010) and years of drought (2011-2016). I used NDVI, EVI, and classified vegetation area shifts from spectral imagery datasets to study how vegetation changes in the Delta during years of drought and normal precipitation. I expected that periods of drought and lower precipitation in the Sacramento-San Joaquin Delta would cause shifts in wetland vegetation. More specifically, during drought I hypothesized a lower mean EVI, lower maximum NDVI, a decrease in area of vegetation cover, and that vegetation patches, or distinct areas of vegetation, would have increased shape complexity and fragmentation. I also predicted that if vegetation shifted in response to drought, years returning to normal precipitation levels would see a return to pre-drought conditions due to the relatively rapid response and recovery of vegetation (US EPA 2002).

METHODS

Study Sites

To determine drought impact on wetland vegetation, I studied four wetland sites in the Delta: two historically unmodified (reference sites) and two restored. Reference wetlands are high functioning wetlands considered natural or close to their natural state and are used as a benchmark to assess success of wetland restoration and mitigation. Restored wetlands on the other hand have been manipulated to improve some aspect of their function, such as conversion from agriculture or altering water flow and channels. The two reference sites were Lower Sherman Island and Brown's Island, and the two restored sites were Kimball Island and Mayberry Farms, all located near the confluence of the Sacramento and San Joaquin Rivers at the mouth of the Delta (Figure 1).



Figure 1. Study Site Locations. Google Earth Imagery of the four wetland study sites located at the mouth of the Delta

Wetland Site Details

Lower Sherman Island

Lower Sherman Island is large wetland at over 3,000 acres and has been a designated wildlife area since 1976. Following 1870s levee failures and flooding, agricultural ventures were abandoned, and Lower Sherman Island has mostly returned to its natural state (Angell 2013) (Table 1).

Brown's Island

Brown's Island is part of the East Bay Regional Parks system. This marsh island is right at the confluence of the Sacramento and San Joaquin Rivers, and never having been drained for agriculture has remained a relatively undisturbed wetland (Angell 2013) (Table 1).

Kimball Island

Kimball Island is the smallest study site, a restored wetland mitigation bank established in 1997 by Wildlands Inc. (Wildlands 1997). Before 1997, Kimball Island was leveed, drained, and used for agriculture but was then restored back to an aquatic, wetland tidal marsh through breaching levees and expanding the island's irrigation channels. Interior channels further from restoration levee breaches experience lower water circulation due to abundant hyacinth congestion (Table 1).

Mayberry Farms

Mayberry Farms is located on Sherman Island and owned by the Department of Water Resources. Before restoration, Mayberry Farms was managed for agriculture and grazing land with constructed levees and drainage. As part of the Subsidence Reversal and Carbon Sequestration Project, the site was restored in 2010 to 192 acres of emergent wetlands and 115 acres of seasonally flooded wetlands (Chamberlin 2008). In efforts to mitigate Delta subsidence, peat soil was excavated to create channels and ponds and then compacted to construct berms and islands among permanently flooded wetlands (Angell 2013) (Table 1).

Table 1. Study Site Descriptions. Locations, size, management history, and site condition descriptions of wetland sites

Site	Location	Size	Management Status	Water	Vegetation
Lower Sherman Island	38°02'25.2"N 121°49'20.6"W	3,100 acres	Reference	Ponds and slough	Invasive submerged aquatic vegetation (SAV) and invasive floating aquatic vegetation, water hyacinth, and Egeria
Browns Island	38°02'15.7"N 121°51'52.4"W	595 acres	Reference	Tidal channel network between marshes and bay	Water hyacinth and parrots feather <i>Schoenoplectus americanus</i> (American bulrush) and <i>Distichlis spicata</i> (salt grass)
Kimball Island	38°01'38.4"N 121°49'01.7"W	105 acres	Restored 1997	Tidal marsh	Tule Dominant with Invasive aquatic plants and SAV, water hyacinth
Mayberry Farms	38°03'12.9"N 121°46'08.3"W	307 acres	Restored 2010	Freshwater	Tule and Cattails

Drought Classification

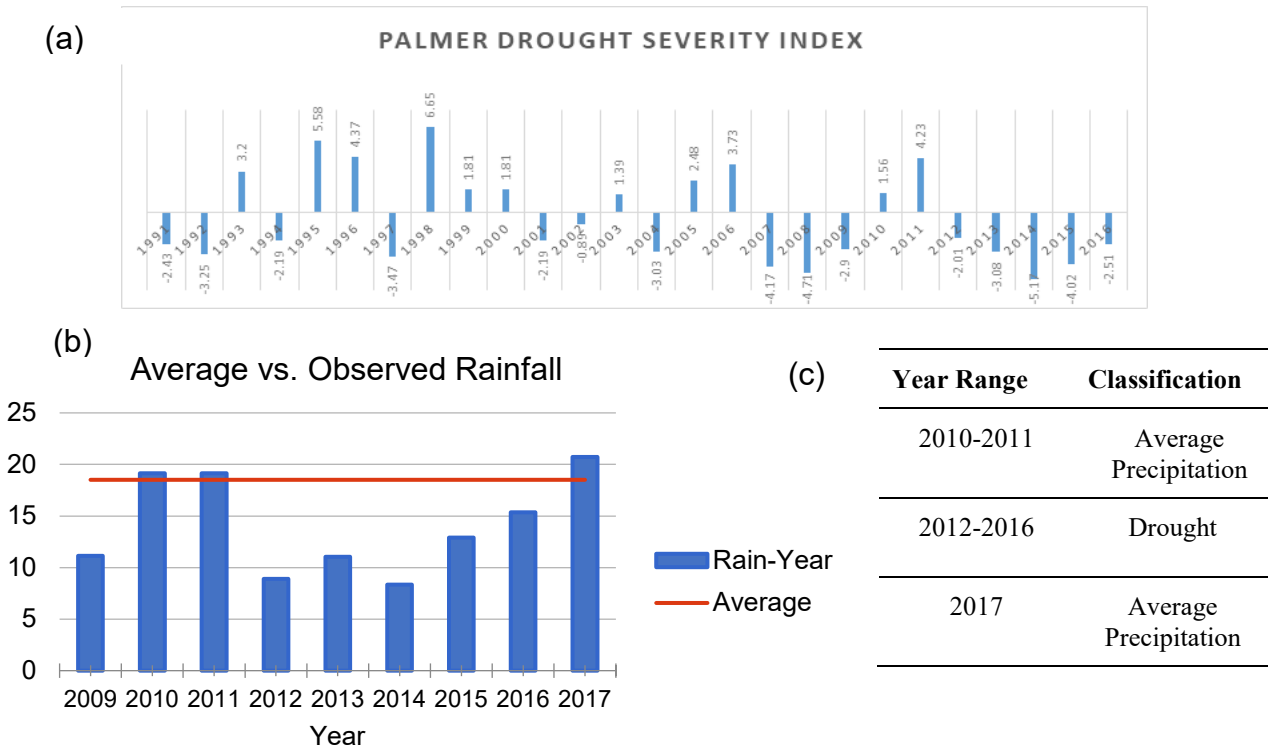


Figure 2. Rainfall Data and Classification. Three resources were used to determine drought years (NOAA 2015; California Energy Commission 2017) . (a) Palmer Drought Severity Index. (b) Graph of compiled precipitation data from Contra Costa County rain-gauges for 2009-2017 rain years (October to September). Compared to “Average” precipitation levels recorded in Sacramento-San Joaquin Delta. (c) Based on Palmer Drought Severity Index, classified year ranges into average precipitation versus times of drought.

To classify years of drought and normal precipitation, I used the Palmer Drought Severity Index and local precipitation information on the Delta data from Contra Costa County water gauges (Figure 2).

Remote Sensing Data Collections

To study vegetation changes at each of the four sites from 2009-2017, I used Landsat 7 satellite imagery in ArcGIS 10.5.1 (ESRI 2017) downloaded from USGS Earth Explorer. Landsat imagery uses the World Geodetic System (WGS) 84 datum and is projected on Universal Transverse Mercator (UTM) WGS 84 at 30 meter resolution (“Landsat Processing Details | Landsat Missions”). To study shifts in vegetation area and characteristics, I used high resolution National Agriculture Imagery Program NAIP imagery from 2012, 2014, and 2016 downloaded from the USDA geospatial database (Table 2). NAIP has 1 meter ground sample resolution and is projected to the Universal Transverse Mercator (UTM) coordinate system and referenced to NAD83 (USGS NAIP 2015).

Table 2. NAIP Capture Dates. NAIP aerial images were taken ranging from late May to the first week of June.

Year	Date of NAIP Imagery Capture
2012	05/20/2012
2014	06/06/2014
2016	05/27/2016 – 05/29 /2016

I created a shapefile of each study site in ArcMap 10.5.1 and used the Extract Mask tool to create individual raster maps for each site and year in Landsat and NAIP.

EVI and NDVI to examine Vegetation Greenness

To measure changes in vegetation greenness or vegetation health and density, I used the Landsat raster of each study site compiled in Google Earth Engine to calculate annual mean

Enhanced Vegetation Index (EVI values) and annual maximum Normalized Difference Vegetation Index (NDVI) (unpublished data by Sophie Taddeo, PhD Student UC Berkeley Landscape Architecture and Architectural Planning). EVI and NDVI are vegetation indices ranging from -1 to 1 that provide estimates of vegetation cover and primary productivity (Table 3). I used both indices for further comparisons.

Table 3. Spectral Indices Formulas. Formulas for spectral vegetation indices NDVI and EVI where Red is red light and NIR is Near-Infrared. Red light = band3, Near-infrared = band4, Blue light = band1. G, C, and L are corrective coefficients for atmosphere reflectance and other noise.

$$NDVI = \frac{(NIR - RED)}{(NIR + RED)}$$

$$EVI = 2.5 * \frac{(NIR - RED)}{(NIR + C_1 * RED - C_2 * BLUE + L)}$$

Live vegetation reflects highly in NIR wavelength and absorbs in red, so higher NDVI and EVI values signify higher vegetated areas. Typically, threshold values of around 0.3 signify presence of vegetation with denser vegetated areas valuing from 0.6 to 0.9 (Jensen 2005). However, wetlands can have smaller thresholds as the presence of water lower NDVI values and canopies may not be as dense. I used the raster calculator tool to quantify changes in NDVI and EVI values across years and the zonal statistics tool to obtain the mean EVI and NDVI values at site locations.

Image Classification

To study shifts in vegetation area and characteristics, I performed image classifications on high resolution National Agriculture Imagery Program NAIP imagery of each site for 2012, 2014, and 2016 capture dates using the image classification toolbar in ArcMap (Table 2). To separate out the three land classes: vegetation, water, and soil, I performed a supervised classification on each image through visual identification of NAIP imagery. Supervised classifications employ training samples, or image portions with a known identity that are used to classify unknown pixels through comparison of their spectral signatures. To assign sufficient training samples for classification, I generated 50 to 60 training samples of each classification class (water, soil, or

vegetation) from NAIP imagery. The resolution of imagery classification did not allow for distinction of plant species, only cover type. After compiling sufficient samples for each study site and year, images from each year were classified into the three categories with the maximum likelihood classification in ArcGIS (Figure 3).

To assess image classification accuracy, I compared the classified images to data derived from high-resolution imagery. For comparison, I generated a set of 300 stratified random points and visually verified with Google Earth imagery that each new generated random point corresponded with the classification category. Then, I used the Confusion Matrix tool in ArcGIS. This tool takes accuracy assessment points to create an error matrix and find overall, producer's, and user's accuracy (ESRI 2017). Because I employed same number and identification techniques for each image's training samples, I only performed accuracy assessments on 2016 classifications for each site and generalized the accuracy across different years. After running the Maximum Likelihood Classification on the images for each year and site, I reclassified the raster imagery and exported the output into Fragstats to calculate landscape metrics (Figure 3).

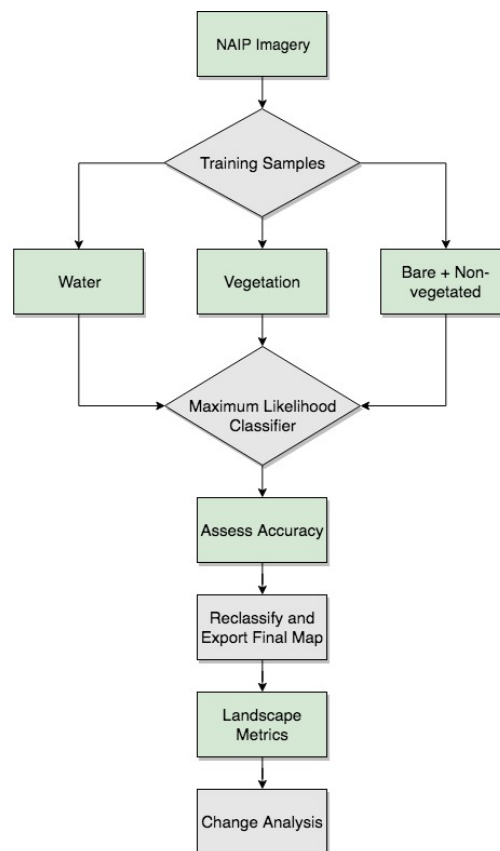


Figure 3. Image Classification Workflow. Steps to classify NAIP imagery and perform Change Analysis.

Data Analysis

Change Detection with Enhanced Vegetation Index and Normalized Difference Vegetation Index

To quantify changes in NDVI and EVI by study site and year, I used the zonal statistic tool in ArcGIS to calculate the maximum, mean, and standard deviation in NDVI and EVI per site. I used Repeated Measures ANOVA to determine if significant differences occurred in EVI from 2009 to 2017 and NDVI in 2010, 2015, and 2017 over changes in precipitation categories.

To visualize areas of NDVI loss and gains, I used Image Differencing Change Detection in ArcMap. I calculated the difference in NDVI values by subtracting the NDVI raster images and examined these changes by setting threshold values of change at ± 0.1 and ± 0.2 ; increases or decreases at these levels would represent significant proportions of mean EVI and NDVI values, which range largely from 0.3 to 0.6. Then, I overlaid the image differencing output onto the 2016 NAIP Imagery for spatial context.

Change Detection Analysis with Image Classifications and Landscape Metrics

Landscape metrics are algorithms that quantify spatial characteristics of classified classes, patches, and landscapes where a patch is a distinct group of pixels. Using the NAIP classifications for each site and year to analyze vegetation patch dynamics, I performed a landscape metric analysis in Fragstats (McGarigal et. al., 2015). To detect changes in the vegetation class at each site, I compared land cover percentages, and area, variation, shape, density, and spatial distribution of vegetation patches per year (Table 4). To test these landscape metrics for statistically significant changes over time, I used repeated measures ANOVA to compare variables across study years for each outcome variable. These methods test whether each site saw significant change in the vegetation land class over years of varying precipitation.

To compare vegetation shifts between sites, I calculated the rate of vegetation cover change from 2012 to 2014 and 2014 to 2016. To visualize change in landscape metrics. I made change detection maps from 2012 to 2016 for each site using post-classification overlay. In ArcMap, I converted the classification output to vector format, merged polygons by land cover classification, and used the Overlay tool (Figure 3).

Table 4. Landscape Metrics Formulas. Landscape metrics as calculated by Fragstats software. Mean Patch size is in units of meters squared.

Percentage of Landscape	$PLAND = P_i = \frac{\sum_{j=1}^n a_{ij}}{A} (100)$
	<p>P_i = proportion of the landscape occupied by patch type (class) i. a_{ij} = area (m²) of patch ij. A = total landscape area (m²).</p>
Number of Patches	$NP = n_i$ <p>n_i = number of patches in the landscape of patch type (class) i.</p>
Mean Patch Size	$MN = \frac{\sum_{j=1}^n x_{ij}}{n_i}$ <p>MN (Mean) equals the sum, across all patches of the corresponding patch type, of the corresponding patch metric values, divided by the number of patches of the same type. MN is given in the same units as the corresponding patch metric.</p>
Patch Density	$PD = \frac{n_i}{A} (10,000)(100)$ <p>n_i = number of patches in the landscape of patch type (class) i. A = total landscape area (m²).</p>
Standard Deviation	$SD = \sqrt{\frac{\sum_{i=1}^m \sum_{j=1}^n \left[x_{ij} - \left(\frac{\sum_{i=1}^m \sum_{j=1}^n x_{ij}}{N} \right) \right]^2}{N}}$
Coefficient of Variation	$CV = \frac{SD}{MN} (100)$

RESULTS

Remote Sensing Classification Accuracy

For every year, the three classified cover categories of water, vegetation, and soil had an overall classification accuracy above 85%, the acceptable assessment threshold (Jensen 2005). Overall classification accuracy for each year's imagery was highest for Mayberry Farms, and

lowest for Kimball Island (Table 5). Misclassification errors occurred most commonly between less green vegetation and non-vegetated areas, and as well as with non-vegetated areas and water boundary regions or mudflats. Classification was most accurate for water and dense vegetation, which had more distinct spectral signatures. There was some speckling and confusion with NAIP's high resolution, however, vegetation cover class had all accuracies above 80%.

Table 5. Accuracy Assessment. Accuracy assessment percentages for each land cover category in 2016 using Error Matrix Tool in ArcMap. Producer's accuracy is the likelihood land cover is classified as such on the output map, and user's accuracy is the percentage of output classification actually present on the ground (Jensen 2005).

	Lower Sherman 2016		Browns Island 2016		Kimball Island 2016		Mayberry Farms 2016	
	Overall Accuracy: 91.7%		Overall Accuracy: 92.7%		Overall Accuracy: 86%		Overall Accuracy: 96.3%	
Class	Producer's	User's	Producer's	User's	Producer's	User's	Producer's	User's
Water	97%	88.8%	92.9%	100%	100%	86.6%	99%	100%
Vegetation	90.8%	99.3%	100%	81.5%	80%	88.2%	93.8%	91%
Soil	83.7%	77.4%	88.3%	98.7%	93%	87.5%	96%	96%

Changes in Annual Mean EVI (Enhanced Vegetation Index)

Across sites, annual mean Enhanced Vegetation Index (EVI) showed a significant net decrease from 2010 (pre-drought) to 2015 [$t(3) = 4.525$, $p = 0.024$], although values did not change significantly year-to-year from 2010 to 2015 [$F(1.5, 4.4) = 2.067$, $p = 0.228$] (Figure 4). Mayberry Farms was restored and flooded in 2010 causing the large dip in EVI values between 2009 and 2011. Meanwhile, Kimball and Sherman Island had small differences in EVI between years in the beginning of the drought (Figure 4). All sites decreased 2013 to 2014 (Figure 4). Values for all sites converged to slightly below 0.3 in 2015, indicating a trend towards average values less dense and green vegetation (see Appendix A Table A1 for EVI values).

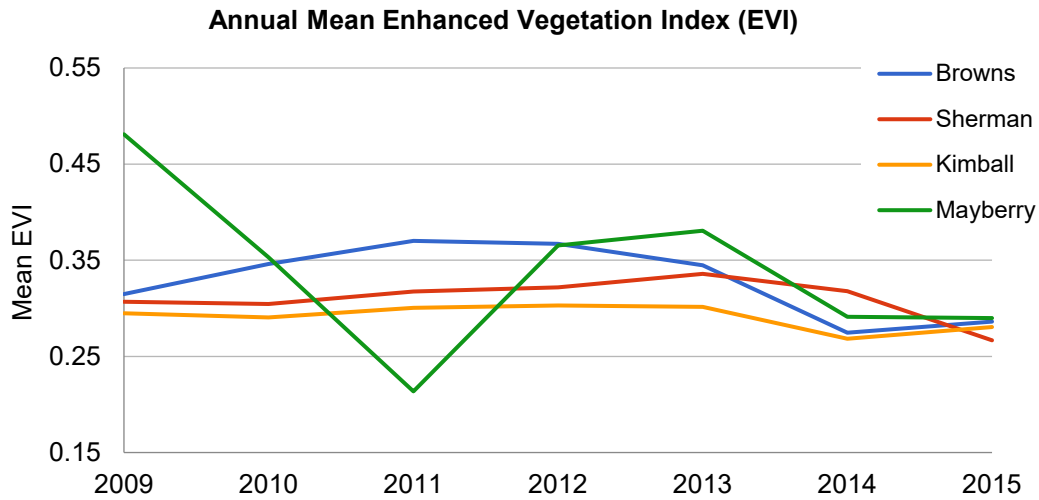


Figure 4. Mean EVI. Changes from 2009 to 2015 in annual mean EVI by site

Changes in Annual Maximum NDVI (Normalized Difference Vegetation Index)

For all four sites, annual maximum NDVI significantly decreased at each interval from 2010, 2015, to 2017 [$F(2,6) = 23.350, p = 0.015$]. Mayberry Farms had a particularly large drop of -23.6% in NDVI from 2010 to 2015 (Figure 5) (see Appendix B Table B1 for NDVI values).

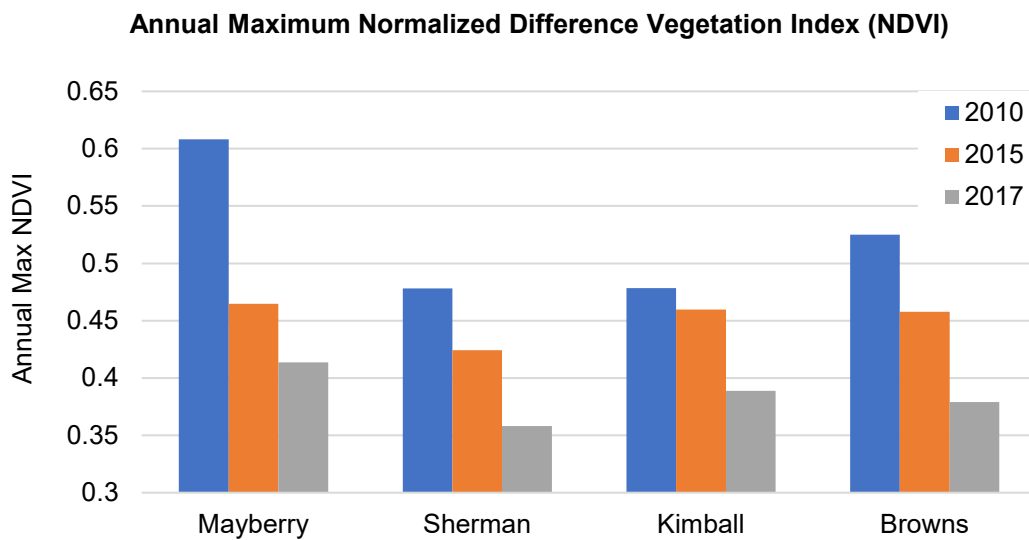


Figure 5. Maximum NDVI. Normalized Difference Vegetation Index 2010, 2015, 2017 by site

From 2010 (pre-drought) to 2015 (middle of the drought) the largest decreases or concentration of red, signifying decreasing NDVI values, occurred in the water on aquatic vegetation, and along

the external and internal edges of the study site at water channels or mudflat regions (Figure 6a). Lower flow and water levels seem to have a more immediate effect in these areas. Mayberry Farms on the east side shows a strong general decrease. Kimball Island on the south side barely experiences change and appears fairly stabilized (Figure 6a). Between 2015 (drought) to 2017 (an above average rainfall year) widespread decreases in NDVI are now concentrated on inland vegetation across all sites and particularly in Lower Sherman Island (Figure 6b).

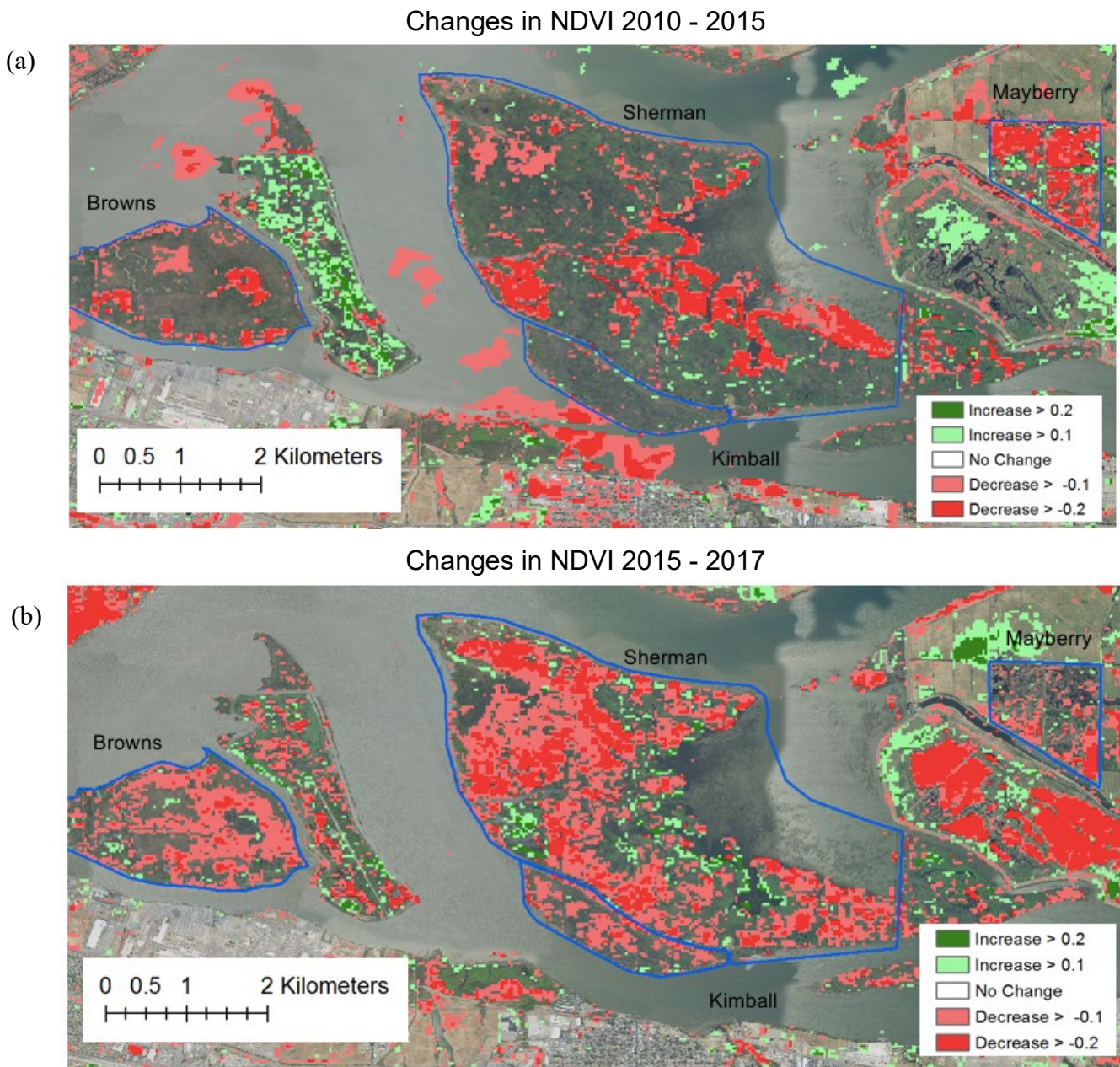


Figure 6. Image Differencing Change Detection of NDVI. Change detection map of maximum NDVI values (a) 2010-2015 and (b) 2015-2017 using thresholds of +/- 0.2 and 0.1 NDVI change.

Site Changes in Vegetation Cover

Vegetation cover area and rate of change at the four sites did not have statistically significant changes across study years [$F(2,6) = 0.74$, $p = 0.929$] however, in general, the percentage of total vegetation cover increased from 2012 to 2016 in all sites except for Mayberry Farms (Figure 7). Vegetation cover changed more quickly from 2012 to 2014 for the two restored sites Kimball and Mayberry, although in opposite directions, and Sherman Island had a large gain in vegetation from 2014 to 2016 (Table 6).

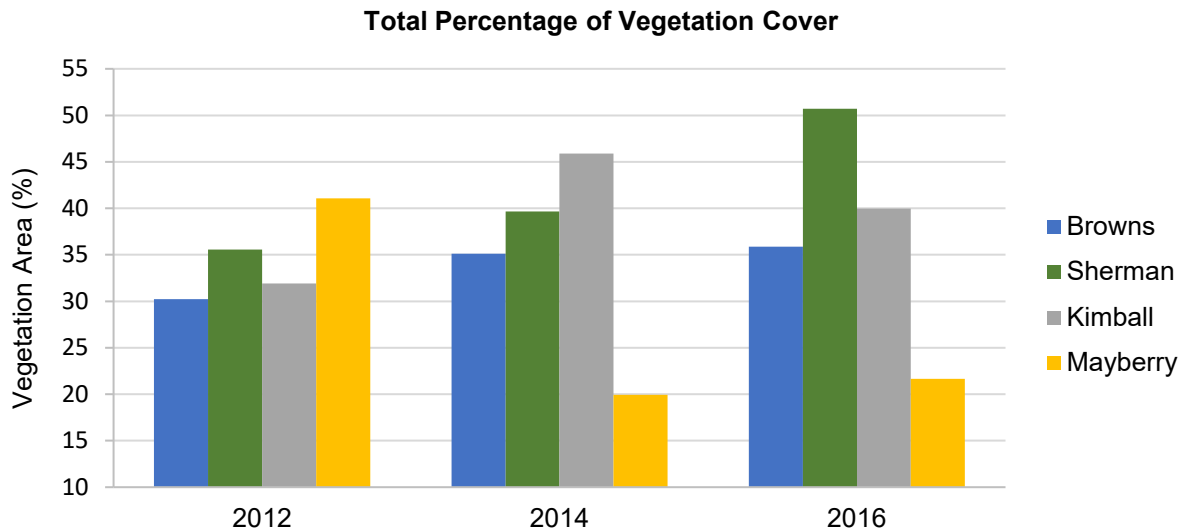


Figure 7. Vegetation Cover Area. The percentage of vegetation class land cover in total site area.

Table 6: Rate of Vegetation Cover Area Change. Rate at which vegetation cover percentage increased or decreased in the two time intervals, from 2012 to 2014 and 2014 to 2016.

Site	2012 - 2014	2014 - 2016
Browns	2.433	0.381
Sherman	2.044	5.524
Kimball	6.981	-2.964
Mayberry	-10.557	0.858

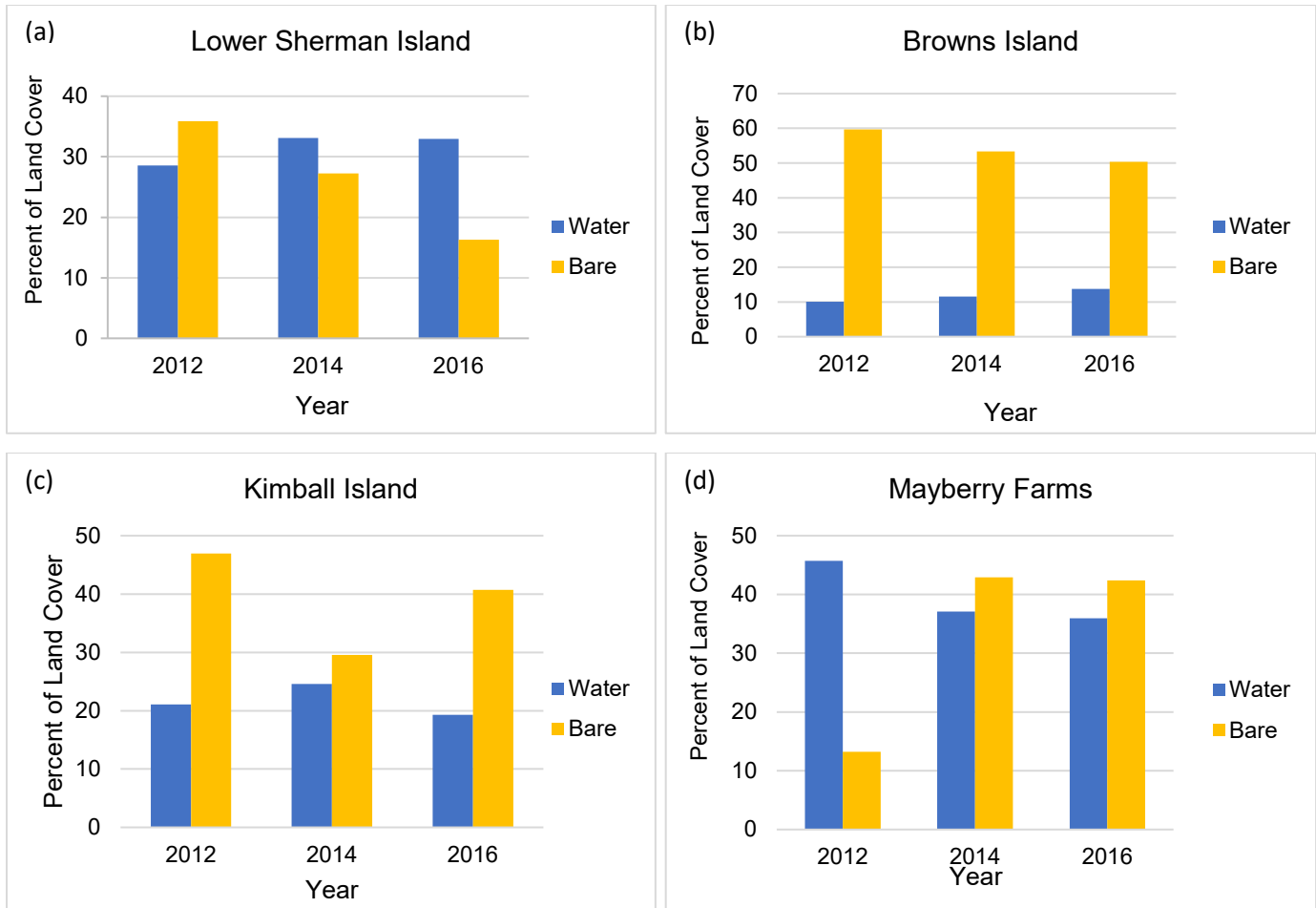


Figure 8. Water and Bare/Non-vegetated Cover Areas. The percentage of water and bare/non-vegetated classes in total site area.

Change detection maps show land cover changes and the different magnitudes and patterns of vegetation losses and gains at each site (Figure 9). Lower Sherman Island sizably increases in vegetation in all areas except for the most northern part of the island (Figure 9a). Browns Island had more concentrated loss at the Southern edge and around the main inner channel (Figure 9b). Widespread vegetative losses can be seen most prominently in Mayberry Farms across the site (Figure 9c). Kimball Island vegetation losses were mostly clustered around inner channels (Figure 9d).

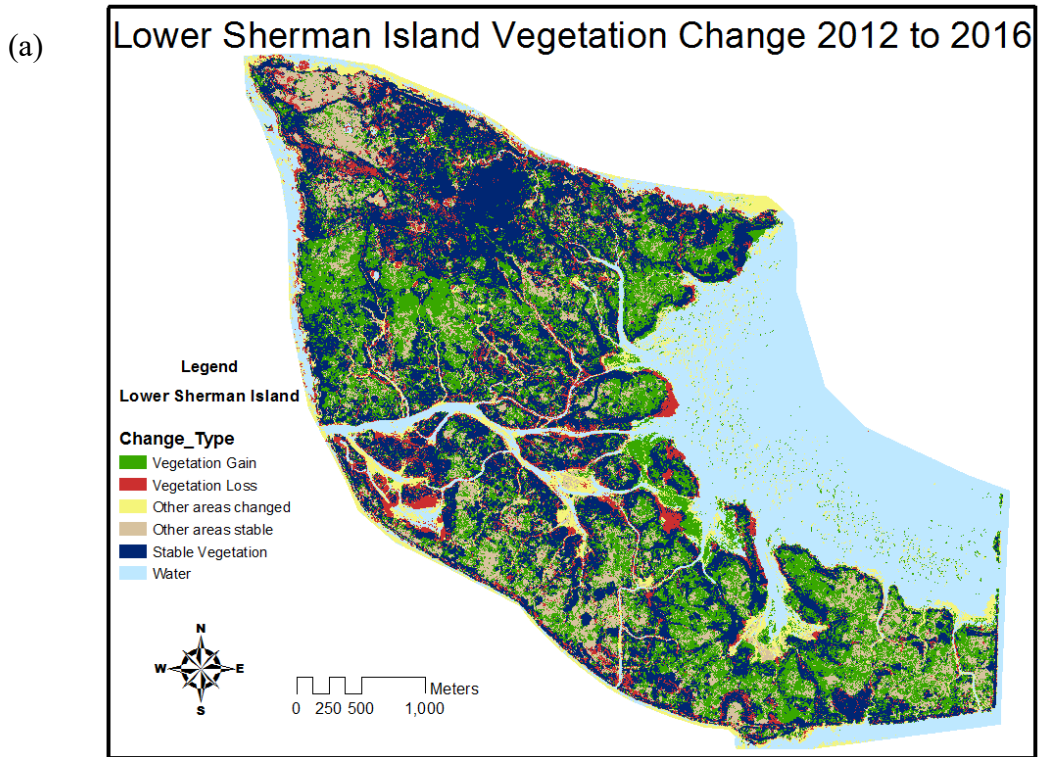


Figure 9(a). Lower Sherman Island Change Detection Map 2012-2016

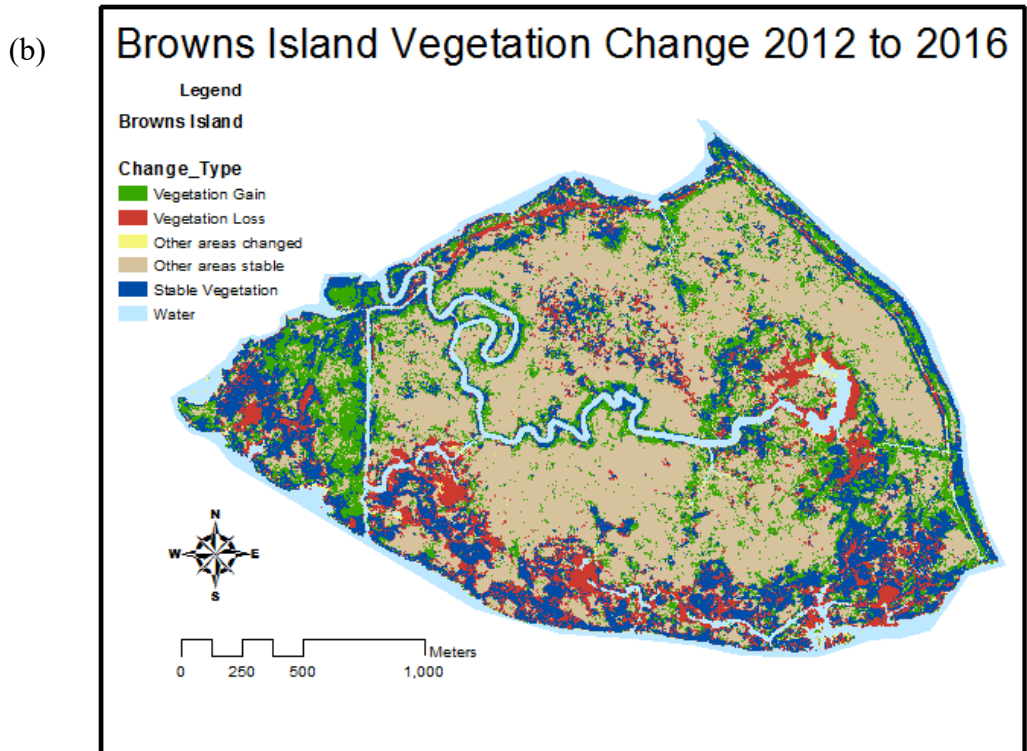


Figure 9(b). Browns Island Change Detection Map 2012-2016

(c)

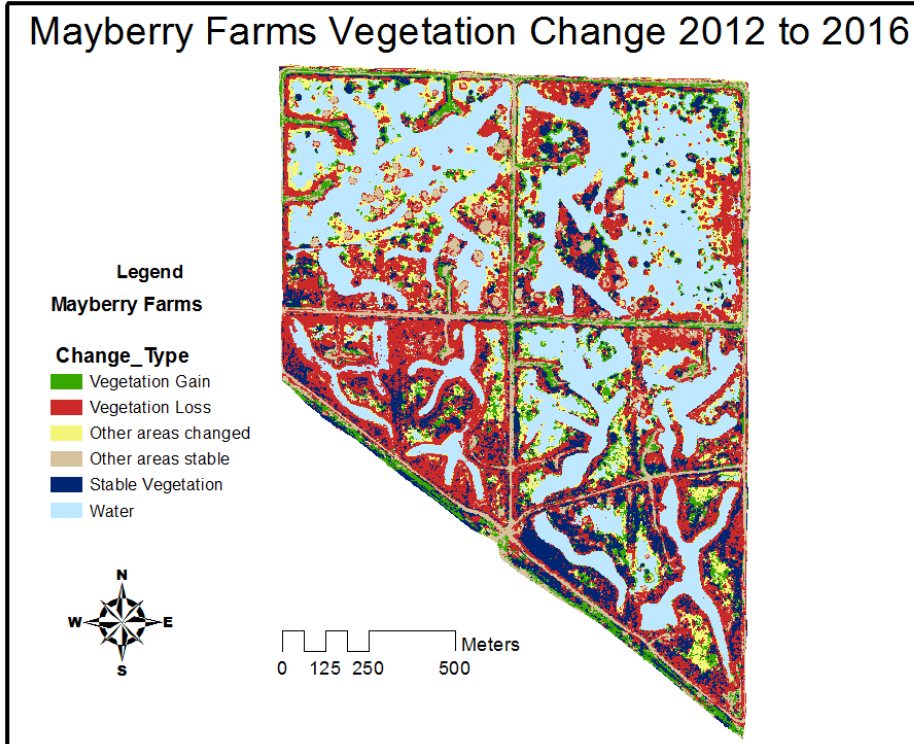


Figure 9(c). Mayberry Farms Change Detection Map 2012-2016

(d)

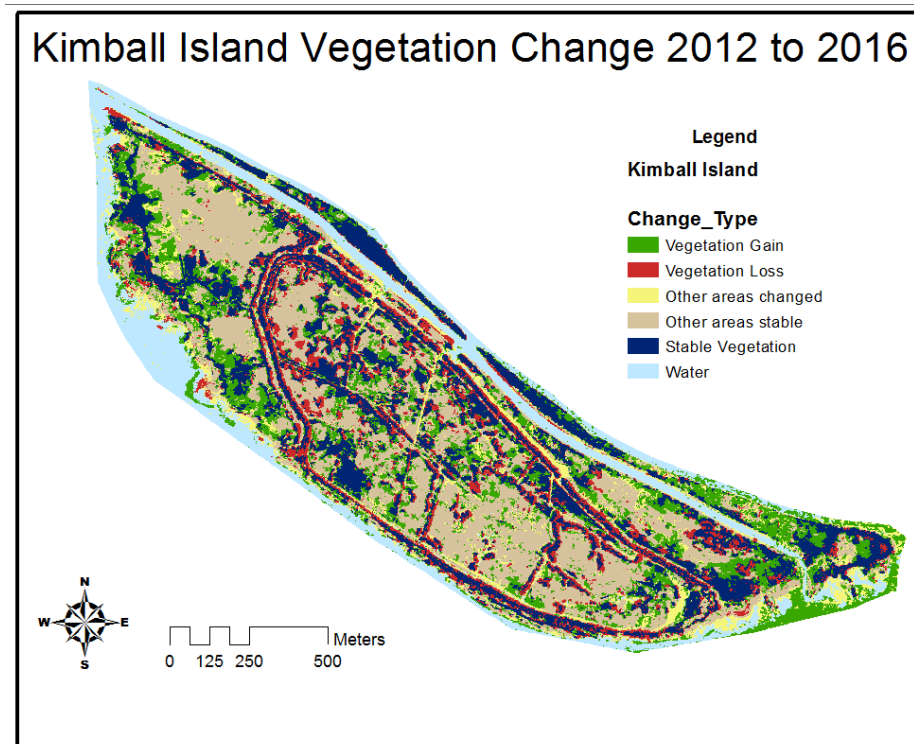


Figure 9(d). Kimball Island Change Detection Map 2012-2016

Landscape Metrics

The landscape metric analysis on the NAIP imagery classification did not reveal a clear trend or singular direction of change among the four study sites nor did analysis of landscape metrics from 2012 to 2016 (Table 7). Although total vegetation area increased for three of the sites, only Sherman Island increased in patch size (Figure 10b) (Table 7). For the four sites, mean patch area [$F(2,6) = 1.763, p = 0.250$] and number of vegetation patches per hectare [$F(2,6) = 4.206, p = 0.072$] did not significantly change from 2012 to 2016 (Figure 10a, 10b). Each site exhibited a net decrease in shape index, indicating a trend towards more compact and less irregular vegetation patch shapes [$F(2,6) = 4.281, p = 0.070$] (Figure 10d). The shape complexity and disaggregation at each site were also dynamic (Figure 10c). In general, Mayberry Farms saw the most variation in terms of increasing number of patches or fragmentation, decreasing vegetation patch area, and disaggregation (Figure 10a-d)(Table 7). Browns Island and Lower Sherman Island, the historic wetland sites, also saw inter-annual variation but at a slower rate (Table 7).

Table 7. Landscape Metrics. Fragstats output of vegetation class statistics for each site and year.

Year	Number of Patches	Mean patch area m ²	Mean Patch Shape	Patch Area Standard Deviation	Patch Area Coefficient of Variation
Sherman Island					
2012	23196	290	1.2021	1.605	5529.522
2014	26666	282	1.2148	2.214	7864.78
2016	19204	499	1.171	3.134	7637.466
Browns Island					
2012	5141	278	1.2755	0.6572	2366.174
2014	19063	87	1.2173	0.3735	4295.028
2016	26222	65	1.2233	0.2916	4514.782
Kimball Island					
2012	2009	284	1.2764	0.5886	2069.835
2014	3822	215	1.2083	0.9338	4346.875
2016	6438	69	1.2588	0.159	2310.478
Mayberry Farms					
2012	1750	449	1.3712	0.8069	1798.275
2014	9857	24	1.2954	0.0198	814.507
2016	9956	42	1.281	0.503	1208.664

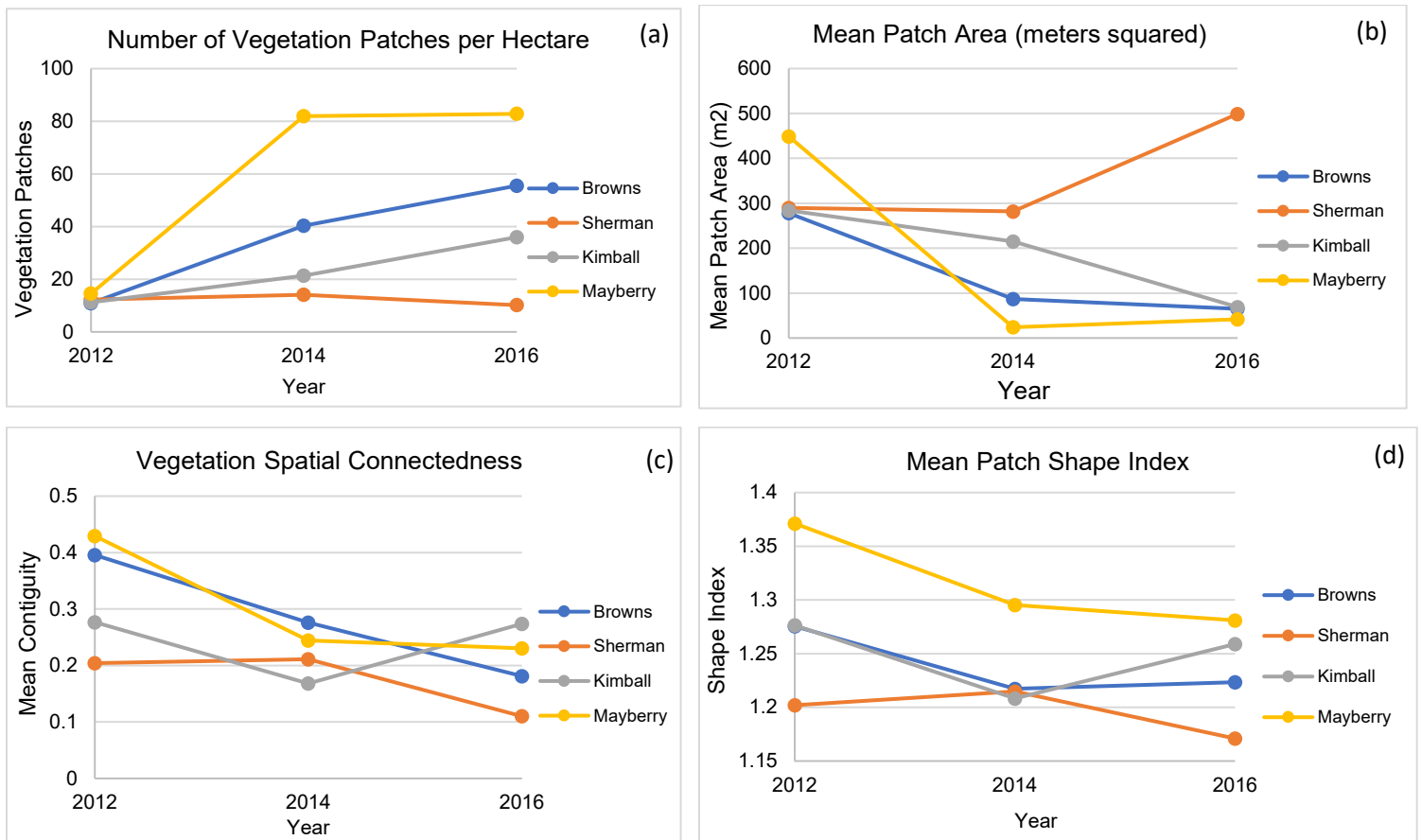


Figure 10. Change in Landscape Metrics. (a) The number of vegetation patches per hectare (b) the mean vegetation patch area in meters squared (c) vegetation spatial connectedness through mean continuity index (d) mean vegetation patch shape index.

DISCUSSION

This study used image classification comparisons and spectral vegetation indices NDVI and EVI to identify changes in vegetation at four Sacramento-San Joaquin Delta wetland sites. In general, none of the study sites were static over the monitoring period. There was variability between study years in both EVI and NDVI, vegetation cover, and vegetation patch characteristics. All sites had significantly decreased in EVI and NDVI values throughout the drought, but only Mayberry Farms showed statistically significant changes in landscape metrics from 2012 to 2016. This variation over time highlights the dynamic nature of these wetland systems and how drought impact differed between sites, particularly Mayberry Farms, the recently restored site. These findings have implications for management practices particularly as drought frequency and

duration increases with climate change. This study also highlights the importance and feasibility of long-term monitoring with remote sensing techniques.

Spectral Vegetation Indices

Mean EVI values for each site decreased overall throughout the drought from 2010 to 2015, and maximum NDVI values for each site decreased across the three rainfall intervals: 2010, 2015, 2017, indicating lower vegetation greenness potentially revealing the effects of less local rainfall. Vegetation greenness was more susceptible to shorter term variation in rainfall, and these EVI values and NDVI values indicate a relatively rapid sensitivity to drought (Jensen 2005). Additionally, in the NDVI Change Detection map from 2015 to 2017, widespread NDVI decreases occur inland, as opposed to 2010 to 2015 decreases along channels and edges. This may indicate that established vegetation further inland takes several years of lower precipitation before noticeable decreases in greenness from drought stress (Figure 6b).

By examining the spectral vegetation indices annually throughout the drought, this study revealed compounding decreases throughout the drought and compares the impact of current year precipitation on vegetation to previous years. From 2012 to 2013, or the first years of drought, only Kimball and Browns Island slightly decreased in mean EVI while Sherman and Mayberry values increased. However, from 2013 to 2014, after a previous and current year of below average rainfall, each site's mean EVI noticeably decreased. Even with above average rainfall in 2017, NDVI was significantly lower than pre-drought levels, and more than a single year was needed for vegetation to recover to pre-drought health and density (Figure 5b). Previous year rainfall is clearly a driver of vegetative conditions, and current year rainfall may not be a good predictor of plant community state (Dudney 2016).

For the EVI time series, short-term effects of drought resembled those of normal inter-annual variability and could be driven by short-term dormancy and mortality of vegetation (Figure 4). The three categorical years of NDVI more clearly highlighted the decreasing trend without the noise of inter-annual variations. Longer-term outcomes would depend on duration of drought, persistence of below-ground life stages of vegetation, and feedbacks on soil, pollinators, herbivores, as drought impacts soil moisture and vegetation biomass and flowering (Copeland 2016).

Post-Classification Comparisons

Limitations of NAIP change detection were largely centered on resolution and classification accuracy and specificity. My classification into three land cover classes of vegetation, non-vegetation, and water, focused on the prevalence or absence of vegetation and did not distinguish between different plant species. Therefore, my results cannot speak to shifts in species dominance, which may be one explanation for the increase in vegetation cover coupled with net vegetation index value losses.

Among the three classes, the classification accuracy assessment showed the highest levels of confusion between vegetation and non-vegetation classes. Particularly for less dense and healthy vegetation, there would be greater spectral confusion between this vegetation and the dead vegetation/bare land cover class. From the 2016 NAIP imagery, Kimball Island in particular had less green vegetation and clear spectral distinction between the two categories, resulting in lower accuracies (Table 5).

With the difficulty of distinguishing between bare soil and “dead” vegetation, these land covers were clumped into one category of bare soil/brown vegetation or non-vegetation, which may explain the significant decrease in “vegetation” cover at Mayberry Farms. The addition of a separate classification for dead vegetation compared to bare ground would add nuance and more information. Mayberry Farms in particular began with high vegetation cover at over 40% in 2012 as a result of recently planted vegetation from 2010 restoration (Figure 7). The substantial decrease in percentage of vegetation area at -10.557% per year from 2012 to 2014, was likely vegetation mortality and a transition to dead vegetation as opposed to a strict conversion into bare ground (Table 6).

Surprisingly, vegetation cover increased throughout the drought. This vegetation cover increase may be due to shifts in growing season for species and peak biomass in response to precipitation changes (Cleland et. al 2007). Lower precipitation decreases snowmelt in the Sierra Nevada, increasing runoff earlier in the winter and reducing freshwater flow in the spring and summer, which could shift biomass levels relative to NAIP image capture dates (Schile et. al 2011).

However, although three sites increased in vegetation cover from 2012 to 2016, both NDVI and EVI significantly decreased. From 2014 to 2016, Lower Sherman Island area of vegetation cover increased at an average rate of 5.524% per year (Table 6). Mean patch area increased and

number of vegetation patches decreased, highlighting a growth and merging of vegetation patches in Lower Sherman (Figure 10a). However, NDVI values indicated lower vegetation health and density throughout the year. This discrepancy suggests that even if vegetation area expanded, these patches were different in character and within-patch density decreased. Possibly, lower-density patches allow for less light competition between plants, resulting in general land cover expansion but sparser patch interiors.

Browns and Kimball Island also had net increases in vegetation cover (Table 4), but vegetation patches decreased in mean area and increased in number per hectare (Figure 10a, Figure 10b). Vegetation cover expansion occurred largely near channels and land edges (Figure 9b, Figure 9d), and with less rainfall and subsequent lower water levels, more mudflat areas were exposed, possibly providing further room for vegetation expansion with seed germination and colonization.

Historic and Reference Site Comparison

Change in wetland vegetation is dynamic and non-linear particularly in restored wetland sites, which may not match characteristics and patterns of reference sites until decades post-restoration (Garbutt and Wolters 2008; Tuxen 2011). Initially, I had intended to compile the results of the two restored sites and the two reference sites to examine compounding differences between the two management categories. However, with high differences in drought response between Mayberry Farms and Kimball Island, it became necessary to examine each site as its own entity.

Mayberry Farms (the most recent restoration from 2010) was an outlier and noticeably impacted by drought beginning in the landscape metrics analysis on 2012. In general, Mayberry Farms showed more drought vulnerability and increased sensitivity to rainfall in terms of vegetation cover, fragmentation, and decreased health and density. Kimball Island, on the other hand, largely matched trends and reactions of historic sites and showed greater stability, suggesting a higher level of establishment 20 years post-restoration. However, the spectral vegetation indices indicate that all sites were vulnerable, impacted by drought, and had net losses in NDVI even in 2017 after a year of higher rainfall.

Methods Review

Wetlands are spatially heterogeneous landscapes and often difficult areas to classify and compare as a result of their dynamic nature and spectral variation, particularly for higher resolution imagery such as NAIP. I used high resolution NAIP imagery from every two years to capture larger trends, as intervals greater than 1 year may be actually beneficial in monitoring efforts to capture larger trends rather than characterize inter-annual variability (Tuxen 2011).

There may also be false changes in established vegetation due to increases in algal coverage, causing an overestimation of vegetation cover in some of the study years. For the coarser Landsat images, EVI served as a useful means to easily detect vegetation and compare site changes across years, although with less accuracy and precision. However, EVI techniques may include spurious algal vegetation in the water, which is also photosynthetically active and can be difficult to distinguish from vascular plants, particularly with spectral indices thresholds like EVI. This highlights the benefits of ground reference data and a further investigation of algal spectral qualities to discriminate between these types of vegetation (Tuxen 2011). From the NDVI change detection maps, decreases in the water and along land areas point to changes in algal communities.

For accurate change detection, studies should have the same spatial and spectral resolution across study years and similar phenological states to increase accuracies in comparisons. Even with all imagery acquired from the last week of May and same seasonal time each year, different phenological states, water levels and mudflat borders, angles of the sun, atmosphere states, and differences in timing of vegetation senescence may have added complications or error to direct year to year comparisons (Tuxen 2011). However to improve accuracy and specific classifications, I created unique training samples for each site and year to address the variability in pixels' spectral signatures resulting from atmospheric conditions, sun position, or water reflectance.

Future Directions

Precipitation has regional scale impacts by altering salinity, timing of river discharge, variation in soil moisture, which in turn, impacts species composition, biomass, and germination (Charles and Dukes 2009). To expand upon this study, next steps include examining other change

metrics of site vegetation such as species level analysis or comparisons of monthly imagery for a more detailed timeline of phenological cycles.

To better understand the larger effects of drought, further studies over more sites would expand understanding of weather-dependent trends. As seen with the different classification outputs from each of the four study sites, including more study sites in the analysis would be required to find general trends and separate out site-to-site variability. Sampling widely throughout the Delta would provide a greater understanding on the relationship between spatial location of sites and influence of precipitation, particularly comparing my freshwater study sites (0.5-5 ppt salinity) to tidal marshes.

Broader Implications

This study contributes to efforts monitoring drought effects on wetland vegetation. Vegetation shifts impact a range of other wetland organisms, indicate an ecosystem's health as a whole, and affect magnitude of carbon sequestration and counteracting land subsidence (Chapple et. al 2017). Considering climate change and projected increases in drought duration, frequency, and severity in Mediterranean climates, understanding responses of wetlands is particularly important (Charles et. al 2009). The change detection output maps, highlight unstable and dynamic regions and general sites trends to use for targeted management. Lower rainfall and hyacinth congestion possibly decreased water flow throughout Kimball Island resulting in vegetation loss along channel edges (Figure 9d), and the southern area of Browns Island experienced concentrated vegetation loss (Figure 9b). Managing to limit vegetation loss under drought conditions at these sites might include clearing Kimball's inner channels or diverting more water to the lower region of Browns Island.

If increased rainfall increases vegetation expansion and influences change, landscape managers can use this information to time restoration efforts with climate or rainfall, snowmelt runoff, and subsequent salinity levels. In addition to rainfall, Delta freshwater input is influenced by groundwater and reservoir flows, water consumption within the Delta, and exports in the southern Delta (Goals Project 2015). Water management for water storage, diversion, and agricultural use must be balanced with the inputs necessary for healthy and robust wetland ecosystems, particularly in years of drought. This study and the results from Mayberry Farms

indicate the importance of prioritizing adequate water inputs especially in the years following restoration.

Continuous long-term site monitoring is required to distill and understand trends and additive effects of consecutive years of drought that may not be apparent on an inter-annual or single site scale. Sustained study identifies underlying causes of vegetation change and “true trends” as opposed to natural variation and “transient trends,” and continued implementation of remote sensing would be an opportunity to better understand this broader landscape (Chappel et. al 2017; Tuxen 2011). In general, site monitoring on a higher temporal and spatial scale improves restoration and management efforts for these important wetland ecosystems.

ACKNOWLEDGEMENTS

Thank you to Sophie Taddeo for being an amazing mentor and guiding me through this whole project. Thank you to Patina Mendez, Kurt Spreyer, Allison, and Leslie for being a dedicated and supportive 175 teaching team and to my peer group Sophia, Ashley, Sarah, and Bessie for their edits and encouragement. This project would also not have been possible without the resources and software at the Berkeley Geospatial Innovation Facility (GIF). Finally, a huge thank you to my wonderful friends and to the best parents anyone could ask for, I will forever be grateful for their love and support.

REFERENCES

- Angell, B., Fisher R., and R. Whipple. 2013. Case Study Report Sherman Island Delta Project. Delta Alliance International Foundation.
<http://www.deltaalliance.org/media/default.aspx/emma/org/10838387/Case+Study+Report+Sherman+Island+Delta+Project.pdf>.
- California Energy Commission. 2017. Climate Tools. Cal-Adapt. cal-adapt.org.
- Chamberlin, J. 2008. Mayberry Farms Subsidence Reversal and Carbon Sequestration Project. State of California Department of Water Resources.
http://www.water.ca.gov/deltainit/docs/mayberry_factsheet.pdf.
- Chapple, D., and I. Dronova. 2017. Vegetation Development in a Tidal Marsh Restoration Project during a Historic Drought: A Remote Sensing Approach. *Frontiers in Marine Science* 4:243.

- Chapple, D. E., Faber, P., Suding, K. N., and Merenlender, A. M. 2017. Climate variability structures plant community dynamics in Mediterranean restored and reference tidal wetlands. *Water* 9 doi:10.3390/w9030209.
- Charles, Heather and Jeffrey Dukes. 2009. Effects of warming and altered precipitation on plant and nutrient dynamics of a New England salt marsh. *Ecological Society of America* 19 <https://doi.org/10.1890/08-0172.1>
- Cleland, E.E., Chuine, I., Menzel, A., Mooney, H.A., Schwartz. 2007. Shifting plant phenology in response to global change. *Trends in Ecology and Evolution* 22:357–365.
- Cloern, J. E., Robinson, A., Richey, A., Grenier, L., Grossinger, R., and K. E. Boyer. 2016. Primary Production in the Delta: Then and Now. *San Francisco Estuary and Watershed Science* 14 <http://dx.doi.org/10.15447/sfew.2016v14iss3art1>.
- Copeland, S. M., Harrison, S. P., Latimer, A. M., Damschen, E. I., Eskelinen, A. M., Fernandez-Going, B., et al. 2016. Ecological effects of extreme drought on Californian herbaceous plant communities. *Ecological Monographs* 86 doi:10.1002/ecm.1218.
- Diffenbaugh NS, Swain DL, Touma D. 2015. Anthropogenic warming has increased drought risk in California. *Proceedings of the National Academy of Sciences* 112:201422385.
- Dudney, J., Hallett, L.M., Larios, L., Farrer, E.C., Spotswood, E.N., Stein, C., and K. N. Suding. 2016. Lagging behind: Have we overlooked previous-year rainfall effects in annual grasslands? *Journal of Ecology* 105 <https://doi.org/10.1111/1365-2745.1267>.
- ESRI. 2017. Accuracy Assessment for Image Classification. ArcMap 10.5. <http://desktop.arcgis.com/en/arcmap/latest/manage-data/raster-and-images/accuracy-assessment-for-image-classification.htm>.
- Environmental Systems Research Institute (ESRI). 2017. ArcGIS Release 10.5.1. Redlands, California, USA.
- Hester, M.W., Willis, J.M., and T. M. Sloey. 2016. Field assessment of environmental factors constraining the development and expansion of *Schoenoplectus californicus* marsh at a California tidal freshwater restoration site. *Wetlands Ecol Manage* 24:33.
- Goals Project. 2015. *The Baylands and Climate Change: What We Can Do. Baylands Ecosystem Habitat Goals Science Update 2015*. San Francisco Bay Area Wetlands Ecosystem Goals Project, California State Coastal Conservancy. http://www.sfei.org/sites/default/files/biblio_files/Baylands_Complete_Report.pdf
- International Water Management Institute (IWMI). 2014. *Wetlands and people*. Colombo, Sri Lanka: International Water Management Institute (IWMI). doi: 10.5337/2014.202.

- Jensen, John R., 2005, *Introductory Digital Image Processing: A Remote Sensing Perspective*, Prentice Hall: Upper Saddle River, NJ, 3rd ed. ISBN 0-13-145361-0.
- Kelly, M., Tuxen, K. A., and Stralberg, D. 2011. Mapping changes to vegetation pattern in a restoring wetland: finding pattern metrics that are consistent across spatial scale and time. *Ecological Indicators* 11 doi:10.1016/j.ecolind.2010.05.003.
- Kirwan, M.L., Murray, A.B., Boyd, W.S., 2008. Temporary vegetation disturbance as an explanation for permanent loss of tidal wetlands. *Geophysical Research Letters* 35 doi:10.1029/2007GL032681.
- Luoama, S. N., C. N. Dahm, M. Healey, and J. N. Moore. 2015. Challenges Facing the Sacramento San-Joaquin Delta: Complex, Chaotic or Simply Cantankerous? *Delta Science Program. San Francisco Estuary and Watershed* 13 <http://dx.doi.org/10.15447/sfew.2015v13iss3art7>.
- Malone, S. L., C. Keough, C. L. Staudhammer, M. G. Ryan, W. J. Parton, P. Olivas, S. F. Oberbauer, J. Schedlbauer, and G. Starr. 2015. Ecosystem resistance in the face of climate change: A case study from the freshwater marshes of the Florida Everglades. *Ecosphere* 6 <http://dx.doi.org/10.1890/ES14-00404.1>.
- McGarigal, K., Cushman, S. A., Neel, M. C., and Ene, E. 2015. FRAGSTATS: spatial Pattern Analysis Program for Categorical Maps. Amherst, Massachusetts, USA. <http://www.umass.edu/landeco/research/fragstats/fragstats.html>
- Millennium Ecosystem Assessment. 2005. *Ecosystems and Human Well-Being: Wetlands and Water Synthesis*. World Resources Institute, Washington, DC.
- Moreno-Mateos D, Power ME, Comín FA, and R. Yockteng. 2012. Structural and Functional Loss in Restored Wetland Ecosystems. *PLoS Biology* 10 doi:10.1371/journal.pbio.1001247.
- Mo Y., Momen B., and S. M. Kearney. 2015. Quantifying moderate resolution remote sensing phenology of Louisiana coastal marshes. Department of Environmental Science and Technology, University of Maryland. *Ecological Monitoring* 312 <https://doi.org/10.1016/j.ecolmodel.2015.05.022>.
- National Drought Mitigation Center. 2017. United States Drought Monitor. <http://droughtmonitor.unl.edu/>.
- NOAA National Weather Service. 2015. Climate Prediction Center - Monitoring & Data: Drought Monitoring. http://www.cpc.ncep.noaa.gov/products/monitoring_and_data/drought.shtml

- Ramsar Convention Secretariat. 2013. The Ramsar Convention Manual: a guide to the Convention on Wetlands (Ramsar, Iran, 1971), 6th ed. Ramsar Convention Secretariat, Gland, Switzerland.
- Schile, L. M., Callaway, J. C., Parker, V. T., and Vasey, M. C. 2011. Salinity and inundation influence productivity of the halophytic Plant *Sarcocornia pacifica*. *Wetlands Ecology and Management* 31 doi: 10.1007/s13157-011-0227-y.
- Touchette B.W., Steudler S.E. 2009. Climate Change, Drought, and Wetland Vegetation. In: Nzewi E. et al. (eds) doi:10.1007/978-0-387-88483-7_32.
- Tuxen, K., Schile, L., Stralberg, D., Siegel, S., Parker, T., Vasey, M., et al. 2011. Mapping changes in tidal wetland vegetation composition and pattern across a salinity gradient using high spatial resolution imagery. *Wetlands Ecology and Management*. 19 doi: 10.1007/s11273-010-9207-x.
- Tuxen K.A., L. M. Schile, M. Kelly, S. W. Stiegel. 2008. Vegetation colonization in a restoring tidal marsh: A remote sensing approach. *Restoration Ecology* 16:313–323.
- U.S. EPA. 2002. Methods for Evaluating Wetland Condition: Using Vegetation To Assess Environmental Conditions in Wetlands. Office of Water, U.S. Environmental Protection Agency, Washington, DC. EPA-822-R-02-020.
- U.S. Geological Survey. 2017. Landsat Processing Details | Landsat Missions. <https://landsat.usgs.gov/landsat-processing-details>
- Wildands Inc. and Sierra View Landscape Inc. 1997. Kimball Island Tidal Aquatic Preserve. CALFED. http://www.calwater.ca.gov/Admin_Record/I-001755.pdf.
- Zedler, J. B. and Suzanne Kercher. 2005. WETLAND RESOURCES: Status, Trends, Ecosystem Services, and Restorability. *Annual Review of Environment and Resources*. 30:39-74.

APPENDIX A: Mean EVI**Table A1:** Zonal Statistics Output of Site Annual Mean EVI from 2009 to 2015

Annual Mean EVI				
Year	Browns	Sherman	Kimball	Mayberry
2009	0.314796	0.306761	0.294981	0.481035
2010	0.346218	0.304542	0.290481	0.352969
2011	0.370168	0.317351	0.300356	0.213622
2012	0.367215	0.321926	0.302971	0.365589
2013	0.344678	0.335866	0.301394	0.380627
2014	0.274645	0.317929	0.268362	0.291141
2015	0.28611	0.266727	0.280438	0.289865

APPENDIX B: Max NDVI

Annual Maximum NDVI				
Year	Browns	Sherman	Kimball	Mayberry
2010	0.524966	0.478181	0.478452	0.608091
2015	0.457733	0.424315	0.459606	0.46479
2017	0.379114	0.358172	0.388904	0.413716

Table B1: Zonal Statistics Output of Site Annual Maximum NDVI in 2010, 2015, and 2017.